THE ARCHIVE OF MECHANICAL ENGINEERING

VOL. LX 2013 Number 3

10.2478/meceng-2013-0023

Key words: optimal control; high speed milling; mobile robots; process surveillance

KRZYSZTOF KALIŃSKI[*], *MAREK GALEWSKI*[*], *MICHAŁ MAZUR* [*]

A SURVEILLANCE OF DYNAMIC PROCESSES IN SELECTED MECHATRONIC SYSTEMS

The paper concerns development of original method of optimal control at energy performance index and its application to dynamic processes surveillance of some mechatronic systems. The latter concerns chatter vibration surveillance during high-speed slender milling of rigid details, as well as motion control of two-wheeled mobile platform. Results of on-line computer simulations and real performance on the target objects reflect a great efficiency of the processes surveillance.

1. Introduction

The problem of effective control has been a subject of study for over one hundred years. Modern methods of control may be very accurate, but they often lack the physical interpretation of the control process itself. They may be also difficult to implement because they require high mathematical skills and deep knowledge of technical aspects of their implementation. On the other hand, many well-known and already applied methods of the optimal control are limited to linear and stationary process [1-3].

The paper presents a method of surveillance of dynamic processes, observed in various mechatronic systems. The method is based on the optimal control at energy performance index [4], whose implementations towards non-stationary and nonlinear process appeared fully successful. The presented method has a physical interpretation because control signals are based on the state of mechanical energy of the system. Moreover, energy of common mechanical or even in some cases mechatronic systems may be computed with the use of well known mathematical formalism. Due to the scalar form of energy, it could be easily manipulated or compared in mathematical sense.

[*] *Gdańsk University of Technology, Narutowicza 11/12, 80-233 Gdańsk, Poland; E-mail: kkalinsk@o2.pl, marg@mech.pg.gda.pl, mazur.m.r@gmail.com*

Moreover, energy can be easily described in the time and frequency domain. Thus, the proposed method is dedicated for application in both domains.

2. Theoretical background

This chapter provides a basic description of the formulated method in generalised coordinates. It is possible to reformulate the presented method with the use of the modal coordinates, as well as – to consider the reduced system. The method of optimal control is also applicable to dynamic systems, whose behaviour is described in hybrid coordinates (i.e. mixed generalised and modal ones), and state ones for continuous and discrete time [4].

The dynamics of linear non-stationary system is expressed by the matrix equation:

$$\begin{aligned} \dot{\mathbf{x}} &= \mathbf{A}\mathbf{x} + \mathbf{D}\mathbf{z} + \mathbf{B}\mathbf{u} \\ \mathbf{y} &= \mathbf{C}\mathbf{x} + \mathbf{w} \end{aligned}, \tag{1}$$

where:

$\mathbf{x} = \begin{bmatrix} \dot{\mathbf{q}}^{*T} & \mathbf{q}^{*T} \end{bmatrix}^T$ – state vector,

$\mathbf{A} = \begin{bmatrix} -\mathbf{M}^{*-1}\mathbf{L}^* & -\mathbf{M}^{*-1}\mathbf{K}^* \\ \mathbf{I} & \mathbf{0} \end{bmatrix}$ – state matrix,

$\mathbf{D} = \begin{bmatrix} -\mathbf{M}^{*-1} \\ \mathbf{0} \end{bmatrix}$ – disturbance matrix,

$\mathbf{B} = \begin{bmatrix} -\mathbf{M}^{*-1}\mathbf{B}_u^* \\ \mathbf{0} \end{bmatrix}$ – input matrix,

$\mathbf{C}$ – output matrix,

$\mathbf{q}^*$ – vector of generalised coordinates,

$\mathbf{z} \equiv \mathbf{f}^*$ – disturbance vector,

$\mathbf{u}$ – control (input) vector,

$\mathbf{y}$ – output vector,

$\mathbf{w}$ – vector of measurement noise,

$\mathbf{M}^*$ – matrix of inertia,

$\mathbf{L}^*$ – matrix of damping,

$\mathbf{K}^*$ – matrix of stiffness,

$\mathbf{B}_u^*$ – matrix of control.

If all components of the generalised coordinates' vector are measured, then: $\mathbf{y} \equiv \mathbf{q}$. All non-potential forces, whose work does not influence the control commands, that is to say vector $\mathbf{f}^*$, are considered as disturbance.

The presented state-space description of dynamic system is a general-purpose one. It can be applied to both linear (stationary and nonstationary) and nonlinear systems.

When we apply the state transition method, the solution to the first matrix equation (1) shall be obtained in following form [5]:

$$\mathbf{x}(t) = \mathbf{\Phi}(t, t_0)\,\mathbf{x}(t_0) + \int_{t_0}^{t} \mathbf{\Phi}(t, \tau)\,[\mathbf{B}(\tau)\,\mathbf{u}(\tau) + \mathbf{D}(\tau)\,\mathbf{z}(\tau)]\,d\tau, \tag{2}$$

where:

$\mathbf{\Phi}(t, t_0)$ is the solution to homogeneous differential equation: $\dot{\mathbf{x}} = \mathbf{A}(t)\,\mathbf{x}$, $\mathbf{x}(t_0) = \mathbf{I}$.

The energy performance index is defined further. It considers kinetic and potential energy of the system with respect to trajectory of the desired motion, as well as – instantaneous energy of the control command. This trajectory is defined by vector of generalised coordinates $\bar{\mathbf{q}}$ and vector of generalised velocities $\dot{\bar{\mathbf{q}}}$. Thus, the performance index has a form [4]:

$$J(t) = \frac{1}{2}\left(\dot{\mathbf{q}}^* - \dot{\bar{\mathbf{q}}}\right)^T \mathbf{Q}_1\mathbf{M}^*\left(\dot{\mathbf{q}}^* - \dot{\bar{\mathbf{q}}}\right) + \frac{1}{2}(\mathbf{q}^* - \bar{\mathbf{q}})^T\,\mathbf{Q}_2\mathbf{K}^*(\mathbf{q}^* - \bar{\mathbf{q}}) + \frac{1}{2}\mathbf{u}^T\mathbf{R}\mathbf{u}, \tag{3}$$

where:

$\mathbf{Q}_1$, $\mathbf{Q}_2$ – matrices of dimensionless weighing coefficients,

$\mathbf{R}$ – matrix of control command effect.

Vector of generalized displacement $\bar{\mathbf{q}}$ is the solution to the matrix algebraic equation:

$$\mathbf{K}^*\bar{\mathbf{q}} = \mathbf{f}_0, \tag{4}$$

where:

$\mathbf{f}_0$– vector of nonpotential generalised forces of the system, which are loads in the desired motion. In particular case: $\mathbf{f}_0 \equiv \mathbf{f}^*$.

Vector of generalized velocities $\dot{\bar{\mathbf{q}}}$ is calculated as time derivative of the $\bar{\mathbf{q}}$ vector.

Matrix $\mathbf{Q}_1$ describes influence of the kinetic energy, which is very important, for example, during the process of unsteady vibration surveillance, while matrix $\mathbf{Q}_2$ – influence of the potential energy, which is essential during the surveillance of the time-delayed closed loop systems' vibration.

Variation of the performance index (3) has the form:

$$\begin{aligned}\delta J = {} & \frac{1}{2}\left(\dot{\mathbf{q}}^* - \dot{\bar{\mathbf{q}}}\right)^T\left(\mathbf{Q}_1\mathbf{M}^* + \mathbf{M}^{*T}\mathbf{Q}_1^T\right)\delta\left(\dot{\mathbf{q}}^* - \dot{\bar{\mathbf{q}}}\right) \\ & + \frac{1}{2}(\mathbf{q}^* - \bar{\mathbf{q}})^T\left(\mathbf{Q}_2\mathbf{K}^* + \mathbf{K}^{*T}\mathbf{Q}_2^T\right)\delta(\mathbf{q}^* - \bar{\mathbf{q}}) + \frac{1}{2}\mathbf{u}^T\left(\mathbf{R} + \mathbf{R}^T\right)\delta\mathbf{u}\end{aligned}. \tag{5}$$

With the use of the following substitutions:

$$\dot{\mathbf{q}}^* = \underbrace{\left[\begin{array}{c|c} \mathbf{I} & \mathbf{0} \end{array}\right]}_{\mathbf{T}_1}\mathbf{x} = \mathbf{T}_1\mathbf{x}, \quad \mathbf{q}^* = \underbrace{\left[\begin{array}{c|c} \mathbf{0} & \mathbf{I} \end{array}\right]}_{\mathbf{T}_2}\mathbf{x} = \mathbf{T}_2\mathbf{x}$$

one obtains:

$$\delta\dot{\mathbf{q}}^* = \mathbf{T}_1\delta\mathbf{x}, \quad \delta\mathbf{q}^* = \mathbf{T}_2\delta\mathbf{x}.$$

Thus, the variation of equation (2) is obtained, i.e.:

$$\delta\mathbf{x} = \int_{t_0}^{t} \mathbf{\Phi}(t,\tau)\,\mathbf{B}(\tau)\,\delta\mathbf{u}(\tau)\;d\tau = \int_{t_0}^{t} \mathbf{\Phi}(t,\tau)\,\mathbf{B}(\tau)\,d\tau\;\delta\mathbf{u}. \tag{6}$$

It is assumed that the control process does not influence the desired trajectory. Thus:

$$\delta\left(\dot{\mathbf{q}}^* - \dot{\bar{\mathbf{q}}}\right) \cong \delta\dot{\mathbf{q}}^*, \quad \delta\left(\mathbf{q}^* - \bar{\mathbf{q}}\right) \cong \delta\mathbf{q}^*. \tag{7}$$

When we compare variation of the performance index to zero and consider relationships (7), Eq. (3) is transformed into the following form:

$$\begin{aligned}\delta J = \Bigg[&\frac{1}{2}\left(\dot{\mathbf{q}}^* - \dot{\bar{\mathbf{q}}}\right)^T \left(\mathbf{Q}_1\mathbf{M}^* + \mathbf{M}^{*T}\mathbf{Q}_1^T\right)\,\mathbf{T}_1 \int_{t_0}^{t} \mathbf{\Phi}(t,\tau)\,\mathbf{B}(\tau)\,d\tau \\ &+ \frac{1}{2}\left(\mathbf{q}^* - \bar{\mathbf{q}}\right)^T \left(\mathbf{Q}_2\mathbf{K}^* + \mathbf{K}^{*T}\mathbf{Q}_2^T\right)\,\mathbf{T}_2 \int_{t_0}^{t} \mathbf{\Phi}(t,\tau)\,\mathbf{B}(\tau)\,d\tau + \frac{1}{2}\mathbf{u}^T\left(\mathbf{R} + \mathbf{R}^T\right)\Bigg]\,\delta\mathbf{u} = 0\end{aligned} \tag{8}$$

After rearrangement of expression (8) we obtain optimal control command:

$$\begin{aligned}\mathbf{u} = -\left(\mathbf{R} + \mathbf{R}^T\right)^{-1} \int_{t_0}^{t} \mathbf{B}^T(\tau)\,\mathbf{\Phi}^T(t,\tau)\,d\tau \Big\{&\mathbf{T}_1^T\left(\mathbf{M}^{*T}\mathbf{Q}_1^T + \mathbf{Q}_1\mathbf{M}^*\right)\left[\dot{\mathbf{q}}^* - \left(\dot{\mathbf{K}}^{*-1}\mathbf{f}_0 + \mathbf{K}^{*-1}\dot{\mathbf{f}}_0\right)\right] + \\ &+\mathbf{T}_2^T\left(\mathbf{K}^{*T}\mathbf{Q}_2^T + \mathbf{Q}_2\mathbf{K}^*\right)\left(\mathbf{q}^* - \mathbf{K}^{*-1}\mathbf{f}_0\right)\Big\}\end{aligned} \tag{9}$$

which minimises energy performance index (3), with respect to time. Eq. (9) is the function of a vector of generalised coordinates $\mathbf{q}^*$, and a vector of generalised velocities $\dot{\mathbf{q}}^*$. Their instantaneous values are computed *on-line*, during the control process performance.

In case of a real control process, control command components are restricted. Taking it into account, one must include restrictions on the components, during its computation:

$$u_i(t) = \begin{cases} u_i(t) & , \quad |u_i(t)| \le U_i \\ U_i sgn\left[u_i(t)\right] & , \quad |u_i(t)| > U_i \end{cases}, \quad i = 1, \ldots, i_u\,, \tag{10}$$

where:

i_u – number of components of the control command vector **u**,

U_i – absolute limit value of component u_i of the control command vector **u**.

The possibility of including constraints during the *on-line* control process is an advantage of the optimal control at energy performance index. The previously formulated methods of the constrained optimal control, on a basis of the Pontryagin's maximum principle, did not have such a feature.

Determination of correct components' values of the matrices $\mathbf{Q}_1$, $\mathbf{Q}_2$ and **R** is an important problem [6]. However, it is not finally resolved yet. It is recommended to avoid casual choice of these values, because of their significant influence on the result of surveillance. The difficulty lies in finding an effective method for searching the space of elements within a huge dimension. One of the proposed solutions is to apply computer simulation method [2]. In order to realize this solution, the following procedure has been proposed [4].

1. Adjusting constant values constraint U_i for the **u** control commands' component u_i.
2. Setting the values of elements of the matrices $\mathbf{Q}_1$, $\mathbf{Q}_2$ and **R**.
3. Computer simulation of the optimal control process at the energy performance index with respect to the desired motion trajectory. Basic stages of the simulation, realized at current instant of time, are:
   – calculation of the optimal control command – equation (9),
   – inclusion of the constant value constraints – relationship (10),
   – solution of the controlled system dynamics equation (1).
4. Evaluation of efficiency of the surveillance. The surveillance efficiency depends on minimisation of vibration level, which is confirmed by the obtained values of indexes. The latter have been defined for particular cases of vibration (e.g. the root mean square index of the time plot, the vibration amplitude index). If the evaluation is unsatisfactory, one must come back to point 2.
5. Evaluation of the control command time plot. The evaluation is justified by necessity of obtaining, during the simulation, such time plot of the control command (e.g. actuator force, spindle speed), which is possible to be performed in real control system. If the evaluation is unsatisfactory, one must come back to point 2.
6. If, despite searching a space of components of matrices $\mathbf{Q}_1$, $\mathbf{Q}_2$ and **R**, the evaluation is still unsatisfactory, one must come back to point 1.

In the case when the size of space of the decisive variables, which are components of matrices $\mathbf{Q}_1$, $\mathbf{Q}_2$ are **R**, is not too large, such a space should be searched successfully with the use of the trial-and-error approach [1, 5].

3. Chatter vibration reduction during High Speed Milling

Milling operations in contemporary production centres are frequently performed with slender ball-end tools. During the cutting process, tool-workpiece relative vibration plays principal role and in certain conditions it may lead to a loss of stability and cause generation of self-excited chatter vibration [4, 7, 8]. There are many different methods for reduction and surveillance of the chatter vibration, i.e.: vibrating cutting [9], control of instantaneous tool-workpiece relative position [10, 11], active damping of the tool or the workpiece [12-14], matching the spindle speed to selected dynamic properties of the system [15, 16], on-line spindle speed optimisation [17]. The group of methods where reduction is obtained thanks to spindle speed variation seems attractive [4, 8, 17]. One of them is the spindle speed optimal-linear control based on the energy performance index principle [18, 19].

The most important reason for vibration occurrence lies in the feedback interaction between the mass-spring-damping system of the milling machine and the milling process. However, the existence of feedback interaction is not sufficient condition for triggering self-excited vibration, it makes the vibrating system potentially unstable. In such a kind of the system, under certain conditions, the feedback interaction may lead to the loss of stability and generation of a limit cycle (i.e. caused by periodic loss of contact between the tool and the workpiece [4, 8]). Relative displacements between the tool and the workpiece during the cutting process imply changes in cutting layer dimensions, which in turn, change cutting forces' values. In return, changing forces cause relative displacements of the tool and the workpiece. Thus, the feedback loop is closed. Additionally, displacement of the tool cutting edge, present in one cutting pass, leaves the trace on the workpiece surface, which interfers with the next pass of the tool cutting edge. This acts as time delay in the feedback loop. This phenomenon is recognised as the most important reason for the tool-workpiece relative vibration and is called the regenerative chatter. The other reasons of the chatter generation are usually of a minor importance.

The analysis of dynamics of a slender ball-end milling of the rigid workpiece has been performed (Fig 1.), taking into consideration the following assumptions:

– In the milling centre structure, the spindle together with the tool and the table with the workpiece are separated into subsystems that experience relative motions. It is shown [18, 19] that those subsystems are essential from the point of view of cutting dynamics, while contribution of the other components of the machine tool structure into tool-workpiece relative vibration is insignificant.

- Only flexibility of the tool is considered. All other components are assumed as perfectly rigid.
- The system is modelled utilising the Finite Element Method (FEM) and is composed of flexible finite element (FFE) no. e and coupling elements (CEs).
  - The FFE is the Euler-Bernoulli bar element [20, 21] fixed at its one end in the tool holder.
  - Coupling elements (CE) are applied in order to idealise the cutting process interaction. They are placed at conventional contact points of the tool edge and workpiece.
- The effect of first pass of the edge along the cutting layer is idealised as proportional feedback, and the effect of multiple passes is idealised additionally as delayed feedback.
- The tool rotates at the spindle speed n.
- The workpiece moves at a constant feed speed v_f.

Coupling elements allow connecting geometrical quantities, such as displacement along principal cutting force, instantaneous cutting layer thickness and instantaneous change in cutting depth, with the force components acting along relevant directions [4, 18, 19]. Coupling elements are described by matrices of the feedback interaction, which are, in general case, non-diagonal. They are mostly defined as appropriate Laplace transfer functions. The latter permit us to consider the desired force and the time-delayed feedback interaction. In the considered case, an influence of angular displacements on cutting forces of CE is neglected. Only longitudinal displacements, as results of the force components acting in orthogonal plane, are included. The component force acting along the tool axis is omitted.

Cutting force in the milling process depends on instantaneous cutting layer thickness, average dynamic specific cutting pressure and cutting depth [4, 18, 19]. For conventional contact point between the tool edge and the workpiece (CE no. l), Cartesian coordinate system y_{l1}, y_{l2}, y_{l3} is introduced in order to define components of the resultant cutting force. Finally, after including the effect of cutting edge being out of the material, when vibration approaches a significant level, several components of instantaneous cutting force are described with the use of the following equations [18, 19]:

$$F_{yl1}(t) = \begin{cases} k_{dl} a_p \left[h_{Dl}(t) - \Delta h_l(t) + \Delta h_l(t - \tau_l) \right] & \text{for} \quad h_{Dl}(t) - \Delta h_l(t) + \Delta h_l(t - \tau_l) > 0 \\ 0 & \text{for} \quad h_{Dl}(t) - \Delta h_l(t) + \Delta h_l(t - \tau_l) \le 0 \end{cases} \tag{11}$$

$$F_{yl2}(t) = \begin{cases} \mu_l k_{dl} a_p \left[h_{Dl}(t) - \Delta h_l(t) + \Delta h_l(t - \tau_l) \right] & \text{for} \quad h_{Dl}(t) - \Delta h_l(t) + \Delta h_l(t - \tau_l) > 0 \\ 0 & \text{for} \quad h_{Dl}(t) - \Delta h_l(t) + \Delta h_l(t - \tau_l) \le 0 \end{cases} \tag{12}$$

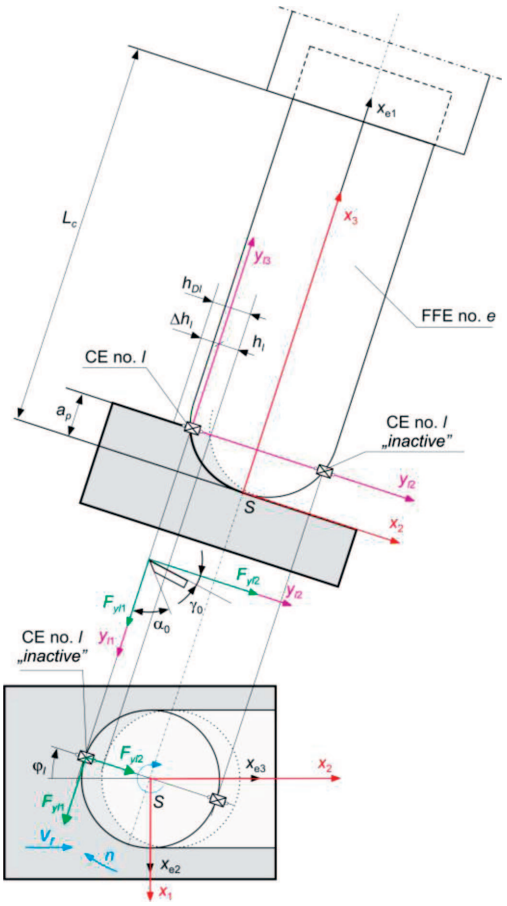

Fig. 1. A scheme of a slender ball-end milling process

$$F_{yl3}(t) = 0 \tag{13}$$

where: k_{dl} – average dynamic specific cutting pressure,
μ_l – cutting force ratio.

Force F_{yl3} =0, because the resultant instantaneous cutting force acts in orthogonal plane.

The regeneration phenomenon makes cutting force dependent on the change in cutting layer thickness due to the pass of the previous cutting edge. This is represented in the model as time delay. Closed loop delayed system can be stable or unstable, depending on a current value of this time delay. In the case of milling, the time delay depends on the difference between angular position of cutting edges and instantaneous spindle speed. This means that it is possible to control stability of the cutting process by the changes of instantaneous spindle speed.

After transformation of displacements to the co-ordinate system x_{1e},x_{2e},x_{3e}, the equation of dynamics has the form [4, 18]:

$$\mathbf{M}\ddot{\mathbf{q}} + \mathbf{L}\dot{\mathbf{q}} + \mathbf{K}^{*}\mathbf{q} = \mathbf{f}^{*}, \tag{14}$$

where:

$$\mathbf{K}^{*}(t) = \mathbf{K} + \sum_{l=1}^{i_l} \mathbf{T}_l^T(t)\,\mathbf{D}_{Pl}\mathbf{T}_l(t),$$

$$\mathbf{f}^{*} = \sum_{l=1}^{i_l} \mathbf{T}_l^T(t)\,\mathbf{F}_l^0(t) + \sum_{l=1}^{i_l} \mathbf{T}_l^T(t)\mathbf{D}_{Ol}\Delta w_l(t-\tau_l),$$

$\mathbf{q}$ – vector of generalised coordinates of the system,

$\mathbf{M}$, $\mathbf{L}$, $\mathbf{K}$ – matrices of inertia, damping and stiffness of the decoupled system (i.e. the slender ball end mill alone),

$\mathbf{F}_l^0(t)$ – vector of desired forces of CE no. l,

$\mathbf{D}_{Pl}$, $\mathbf{D}_{Ol}$ – matrices of proportional and delayed feedback of CE no. l,

$\Delta\mathbf{w}_l(t)$ – vector of deflections of CE no. l for time-instant t,

$\Delta\mathbf{w}_l(t-\tau_l)$ – vector of deflections of CE no. l for time-instant t-τ_l.

$\mathbf{T}_l(t)$ – transformation matrix; time-dependent, because edges of the tool change their positions ourselves.

Because it was assumed that cutting process is performed at time-varying spindle speed $n = n(t)$, the time-delay τ_l for edge no. l becomes a function of instantaneous spindle speed n, i.e. $\tau_l = \tau_l(n)$. It is shown [4, 18] that cutting at changing spindle speed can be described by dynamic equation of the controlled system, i.e.:

$$\mathbf{M}\ddot{\mathbf{q}} + \mathbf{L}\dot{\mathbf{q}} + \mathbf{K}^{*}(t)\,\mathbf{q} = \mathbf{f}^{*} + \mathbf{B}_u\mathbf{u}, \tag{15}$$

where matrix of control is:

$$\mathbf{B}_u(t) = \sum_{l=1}^{i_l} \mathbf{T}_l^T(t)\,\mathbf{D}_{Ol}\Delta\dot{w}_l\left(t - \int_{\phi_l-\phi_{0l}}^{\phi_l} \frac{60}{2\pi}\cdot\frac{d\phi}{n(\phi)}\right)\cdot\left[-\frac{\Delta t}{n(\phi_l)}\right], \tag{16}$$

where (Fig. 1):

ϕ_l – instantaneous angular position of CE no. l,

ϕ_{0l} – the difference between angular position of CE no. l and CE no. l-1.

Next, the energy performance index is defined as in chapter 2 of this paper. In order to minimise vibration level during cutting with variable spindle speed n, the performance index (3) should be minimised, due to instantaneous speed change δn. It implies that :

$$\mathbf{u} \equiv \delta n. \tag{17}$$

The optimal control command has the form [4, 18]:

$$\mathbf{u} \equiv -\mathbf{R}^{-1} \int_{t_0}^{t} \left[\begin{array}{cc} \mathbf{B}_u^T(\tau) & \mathbf{0} \end{array} \right] \mathbf{\Phi}^T(t,\tau)\, d\tau \left\{ \mathbf{T}_1^T \mathbf{M}^T \mathbf{Q}_1^T \dot{\mathbf{q}} + \frac{1}{2} \mathbf{T}_2^T \left(\mathbf{K}^* \mathbf{Q}_2^T + \mathbf{Q}_2 \mathbf{K}^{*T} \right) \left(\mathbf{q} - \mathbf{K}^{*-1} \mathbf{f}_0 \right) \right\} \tag{18}$$

where:

$\mathbf{\Phi}(t, t_0)$ – solution to homogeneous equation $\dot{\mathbf{x}} = \mathbf{A}(t)\,\mathbf{x}, \quad \mathbf{x}(t_0) = \mathbf{I}$,

$\mathbf{A}$(t) – state matrix of the system.

It means that, due to (17), the spindle speed optimal control depends upon instantaneous change δn in spindle speed $n(t)$, being introduced as a command.

Unfortunately, if (18) is applied directly, the spindle speed has a tendency to grow up to infinity. In order to limit this effect, the idea of optimal-linear spindle speed control has been incorporated [18, 19]. After reaching the allowed maximum value n_{max}, the spindle speed is linearly changed down to nominal value n_0. Additionally, simulations have shown that optimal spindle speed programmes have often a shape of repeating triangle-like segments and, for practical reasons, can be substituted by programmes built of repeating triangle segments. The parameters like nominal and maximum spindle speed and speed raise and fall times are chosen according to the results of simulations for optimal spindle speed programme.

The presented approach is applied for chatter vibration reduction on the Alcera Gambin 120CR milling machine equipped with the S2M electrospindle, which can achieve revolution speed up to 35000 rev/min. Displacements of the rotating tool are measured in 2 orthogonal directions. Spindle speed is also measured. A heart of the whole system is a laptop computer equipped with a digital acquisition card. High speed machining of aluminium alloy EN AW 2017A, carbon steel C45, and bronze CC331G were performed using long, slender ball-end mill Fette 16×160.

Simulations showed that variable spindle speed with the speed switching every 0.3 s÷0.5 s allows a significant reduction of chatter vibration. However, experiments revealed that time between switching shorter than 0.4 s is too short, and the desired spindle speed is not approached. Consequently, two variable spindle speed programs are chosen for realisation:

Z04 – at rising and falling time 0.4 s,

Z05 – at rising and falling time 0.5 s.

Experiments for constant speed (15000 rev/min and 16500 rev/min) are also conducted in order to obtain the reference data.

Some results for the aluminium alloy full-immersion ball end milling are presented in Fig 2. In the case of constant spindle speed 15000 rev/min, strong chatter vibration occurred (Fig. 2a, frequency 808 Hz). Application

of changing spindle speed programme caused reduction of maximum amplitude of chatter vibration in the spectrum up to 68% (in comparison with cutting at constant spindle speed 15000 rev/min) (Fig. 2b). The RMS value of tool displacement is also reduced (Fig. 3a). The results for all three tested materials are presented in Figs. 3, 4 and 5.

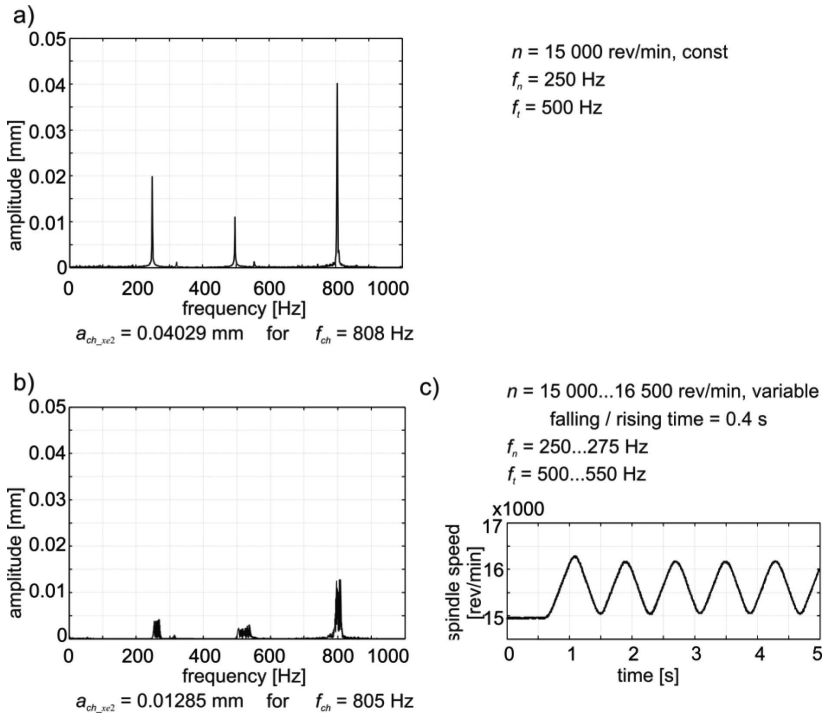

Fig. 2. a) Tool-workpiece relative displacement spectrum for cutting with constant spindle speed b) Tool-workpiece relative displacement spectrum for cutting with variable spindle speed programme which is shown in c); f_n – spindle speed frequency, f_t – cutting edge passing frequency

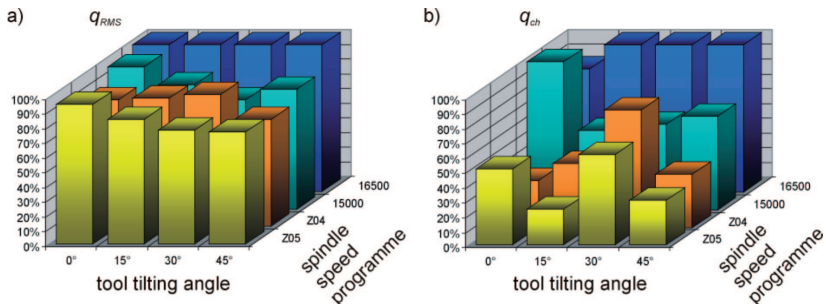

Fig. 3. a) RMS values of tool displacement along the x_{e2} axis and b) maximum amplitude of the chatter spectrum for different spindle speed programmes and tool tilting angles; 100% represents the maximum of displacement's RMS value or chatter spectrum amplitude value for a given tilting angle; full-immersion ball end milling of aluminium alloy EN AW-2017A

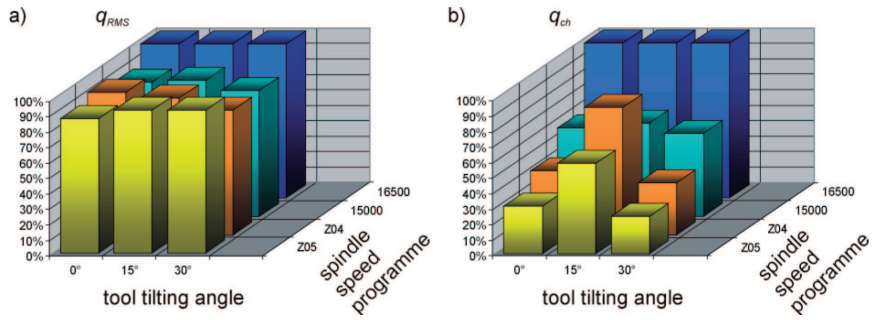

Fig. 4. a) RMS values of tool displacement along the x_{e2} axis and b) maximum amplitude of the chatter spectrum for different spindle speed programmes and tool tilting angles; 100% represents the maximum of displacement's RMS value or chatter spectrum amplitude value for a given tilting angle; full-immersion ball end milling of steel C45

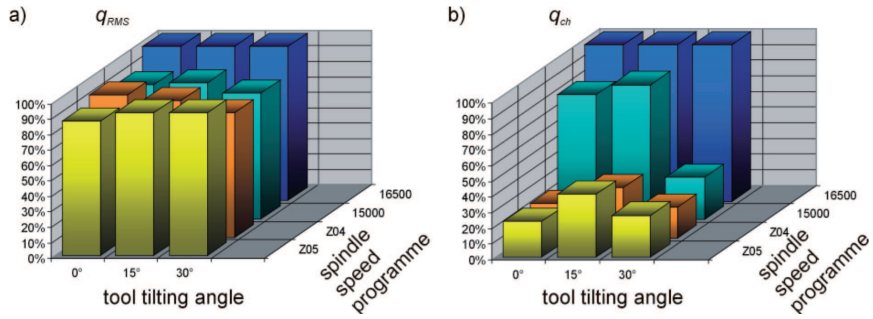

Fig. 5. a) RMS values of tool displacement along the x_{e2} axis and b) maximum amplitude of the chatter spectrum for different spindle speed programmes and tool tilting angles; 100% represents the maximum of displacement's RMS value or chatter spectrum amplitude value for a given tilting angle; full-immersion ball end milling of bronze CC331G

4. Two-wheeled mobile platform

Nowadays, mobile robots are becoming popular in many possible applications. They are commonly used at every modern war theatre. Their use in areas where human presence is not recommended (i.e. due to lethal level of radiation) is also of utmost importance. Moreover, mobile robots become useful in making some mundane works (e.g. cleaning the rooms etc.). In future, due to more accurate and efficient methods of functioning control, they may become popular and utile in new areas of possible activities.

This chapter presents application of the optimal control method at energy performance index to surveillance of the movement of the two-wheeled mobile robot, which is also called: the mobile platform. The presented algorithm of control is dedicated for the use at a low level control, by that we mean that the subject of control is the best possible realization of the desired trajectory

by the mobile platform. High level of the control (e.g. path planning) requires more sophisticated algorithms.

Two-wheeled mobile platforms are ones of the most popular constructions, which have the following advantages.

– They are not complicated and relatively not expensive.

– They express good manoeuvrability.

– They are robust and quiet, especially when compared with platforms equipped with special wheels.

– They are easy to control and energy effective.

Among some disadvantages, one must notice:

– existence of nonholomic constraints. It is not possible to move and rotate freely in the same time when moving in the plane, although it is still possible to achieve every position and orientation in that plane if there are not any other geometrical constraints (e.g. wall);

– possible application only for even, flat surface;

– low speed, small mass and small capacity of loading.

A significant advantage of the presented method of optimal control is the ability to provide, within a very short time, the optimal control command whose value is based on the dynamic model of the controlled two-wheeled mobile platform [21]. The control signals tend to be accurate, so the realization of the given trajectory by the real robot is very smooth. The time needed for reaction is small; thus the errors have no tendency to approach significant values. In many cases of mobile platforms application, a state vector for the needs of motion control is estimated in indirect way, with the use of odometers' techniques and encoders' measurements. The risk of slippages is limited by efficient minimization of the errors during the movement, which can be considered as further improvement of overall performance of the mobile platform. Here the performance improvement of the two-wheel mobile platform's movement is achieved in an indirect way: the risk of slippage is assessed and reduced during simulation process in the first step, and – by obtaining low errors level during realization of the trajectory by the real platform, in the second step of investigation.

In Fig. 6 is presented calculation model of two-wheeled mobile platform. It is equipped with two driving wheels 1 and 2, supported in rigid frame 4. The wheels, whose radiuses are equal (i.e. $r_1 = r_2 = r$) are driven through planar gears by two independent DC motors 5. The slave wheel 3 has a smaller radius r_3 and is purposed as third point of supporting the platform. It has the ability of rotating freely and can take any orientation, together with the robot frame. It is assumed that the robot moves over flat, horizontal surface without slippage and the wheels and other parts of the robot are not subject to any deformations during the movement.

If these assumptions are fulfilled, then the investigated system is cramped with non-holonomic constraints. In this case, it is more convenient to operate with generalised velocities, instead of generalised coordinates, in order to solve the problem of kinematics of two-wheeled mobile robot [22]. This limitation is considered during control of two-wheeled mobile platform. Special mathematical formalism must be used to describe the problems of dynamics of the investigated non-holonomic system. In the thesis [23], one introduces a model based on the Appell-Gibbs equations. Mathematical model of two-wheeled mobile platform is strongly nonlinear. Thus, surveillance of the movement of such a platform is not a trivial task, because of nonlinearities and kinematic constraints between instantaneous velocities of the chosen characteristic points.

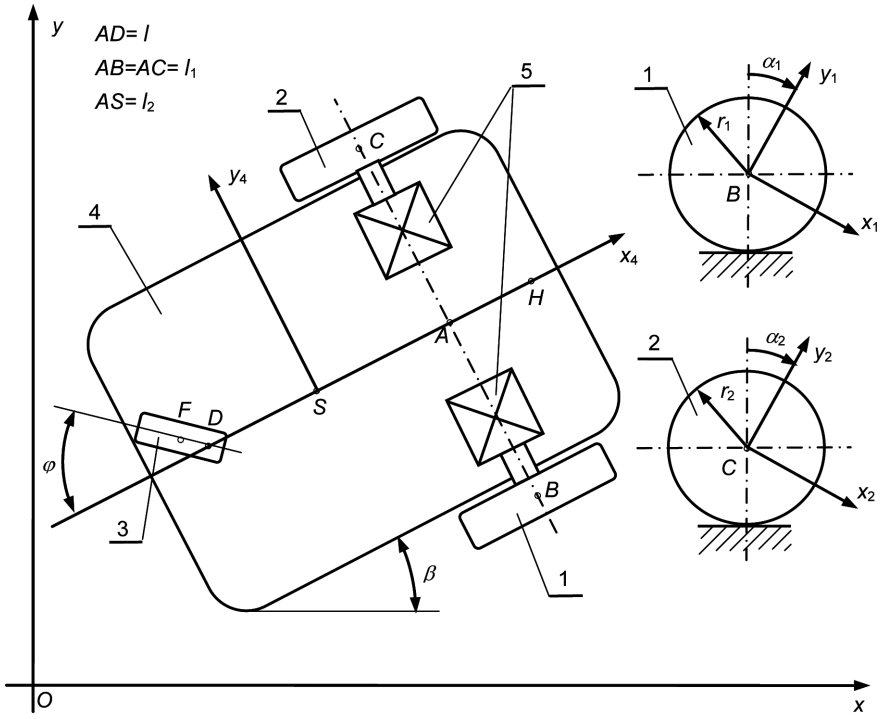

Fig. 6. Model of two-wheeled mobile platform

Conventional point H of the platform is considered in order to define a path, along which the point should move during the platform's motion. Due to significant errors in following the path, the components of instantaneous velocity of this point $\dot{x}_H$ and $\dot{y}_H$ must be modified in such a way that compensation of the errors is assured. For this reason, projections of the position errors on the axes of global coordinate system $\bar{x}_H - x_H$ and $\bar{y}_H - y_H$ are

divided by time-interval Δt during which the error can be corrected. Thus, we obtain correcting velocity components as follows:

$$\begin{aligned} \dot{\hat{x}}_H &= \frac{\bar{x}_H - x_H}{k \cdot \Delta t} \\ \dot{\hat{y}}_H &= \frac{\bar{y}_H - y_H}{k \cdot \Delta t} \end{aligned} , \tag{19}$$

where $\bar{x}_H, \bar{y}_H$ – Cartesian coordinates of the defined position of characteristic point H,

x_H, y_H– Cartesian coordinates of actual position of characteristic point H,

k – experimental scaling factor [23].

The obtained additional velocity components of the characteristic point H allow us to define additional angular velocities of the driving wheels, by solving the problem of the inverse kinematics [21, 23].

For the sake of good efficiency of the motion surveillance, we need to sum the correcting velocity components (19) with those obtained from the problem of kinematics for the desired trajectory. The superposition principle is not valid in non-linear systems. Thus, computation should be performed only for an adequately short period of time. Without making a great error, it is allowable to consider that motion parameters are not changing during the period of the assumed sampling time [21, 23].

The investigated mobile robot moves over a horizontal surface. Thus, potential energy of the robot does not change in time. Here is defined the energy performance index (3), which refers to the time changes of only kinetic energy of the system [23]:

$$J(t) = \frac{1}{2}(\dot{\mathbf{q}} - \dot{\bar{\mathbf{q}}} - \dot{\hat{\mathbf{q}}})^T \mathbf{Q}_1 \mathbf{M}^* (\dot{\mathbf{q}} - \dot{\bar{\mathbf{q}}} - \dot{\hat{\mathbf{q}}}) + \frac{1}{2}\mathbf{u}^T \mathbf{R}\mathbf{u} \tag{20}$$

where: $\dot{\hat{\mathbf{q}}}$ – vector of the correcting generalised velocities, which result from differences between actual and desired position of the mobile platform, divided by the k– scaled assumed time-step.

Further, we consider a system with kinematics constraints. For such a system, it is possible to define variations of generalised velocities. We obtain an optimal control command within sampling time Δt (compare with Eq. (9)) in the following form:

$$\mathbf{u} = -(\mathbf{R}+\mathbf{R}^T)^{-1} \int_t^{t+\Delta t} \mathbf{B}^T(\tau)\, \mathbf{\Phi}^T(t,\tau)\, d\tau \cdot \mathbf{T}_1^T (\mathbf{M}^{*T}\mathbf{Q}_1^T + \mathbf{Q}_1 \mathbf{M}^*)(\dot{\mathbf{q}} - \dot{\bar{\mathbf{q}}} - \dot{\hat{\mathbf{q}}}). \tag{21}$$

For the purpose of computer simulation and control of the real two-wheeled mobile platform, we developed the authorial computer programs,

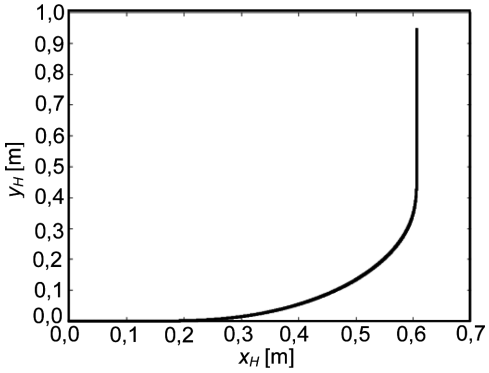

Fig. 7. Path of the point H

written in the C code. The simulation is realized for the path presented in Fig. 7. Firstly, the robot has to accelerate from standstill to the desired velocity v_A =0,1 m/s of the characteristic point A along a straight line, and then the robot has to move along a curve and a straight part of the path. The curve consists of two fragments of clothoids at its beginning and end, and one fragment of circle having constant radius. The fragments of clothoids are used to assure a smooth path and guarantee continuous centrifugal accelerations.

Fig. 8 shows that the course of orientation angle β of the mobile platform with optimal control is very good. Errors are very small and they approach zero by the end of simulation. Other observed courses of important quantities (i.e. velocity of characteristic point A or position of point H) are also very good. The errors of orientation angle β should be small all the time and their fast minimization is very important for movement stability of the two-wheeled mobile platform.

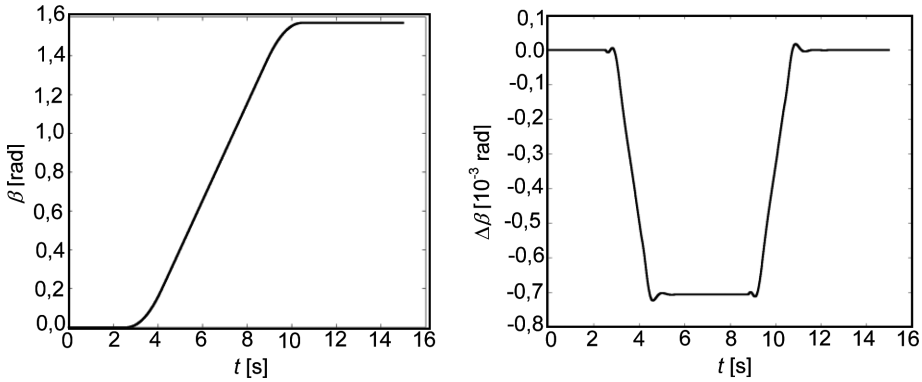

Fig. 8. Course of orientation angle β and error of the orientation angle $\Delta\beta$

Fig. 9 shows two-wheeled mobile platform designed and assembled for the test of the presented control algorithm [23]. During the tests, the platform

was running autonomously. The proposed control algorithm is implemented in the 32bit ARM microcontroller of the platform.

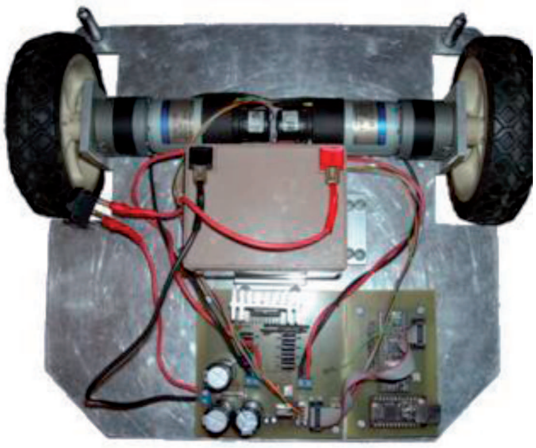

Fig. 9. The designed mobile platform

The tests of the optimally controlled two-wheeled mobile robot at energy performance index are performed for various trajectories. Here is presented a modified trajectory (Fig. 10), with respect to one of the simulation (Fig. 7). A supplementary second curve is added in opposite direction and the final straight line is shortened to capture orientation errors after the final curve. Direct and indirect (incremental) measurements are done for the final position (Fig. 11) and orientation of the mobile platform. There is a very good coincidence between the final position measured in direct and in indirect way. The measured trajectory of the characteristic point H is very close to the desired trajectory. It is shown that the platform moves very precisely along the trajectory. As a reference method of the control, we used the method based on application of the two PID controllers, i.e. the first one for compensation of linear velocity errors, and the second one – for minimisation of angular velocity errors. The only reason for choosing the PID controllers as the reference method is their popularity in the mobile robotics. However, due to an intensive change of poles during the platform motion, it is very difficult to determine correct values of the PID parameters. Hence, the authors adjusted the best set of parameters applying the trial-and-error method. The obtained results are applied for comparison with the results of the optimal control at energy performance index.

The quality of the presented method of control is much better than the reference one, which is not so accurate and due to significant level of errors during realization of the desired trajectory and the existence of slippages that creates a serious problem.

The presented method for low level control of two-wheeled mobile platform appears to be very effective. This conclusion is supported by the following arguments.

– During simulation, the achieved trajectories are very accurate.

– The presented algorithm seems to be practically stable, because the errors are eliminated and the desired trajectories remain close to the real ones during the simulation time.

– The results of the tests on a real object appear to be very good.

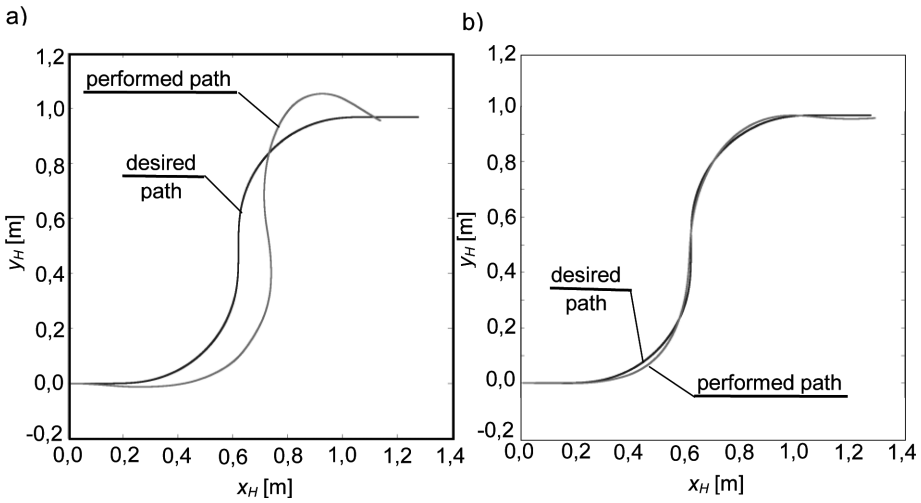

Fig. 10. Desired and performed path of point H of the mobile platform: a) the PID control, b) optimal control at energy performance index

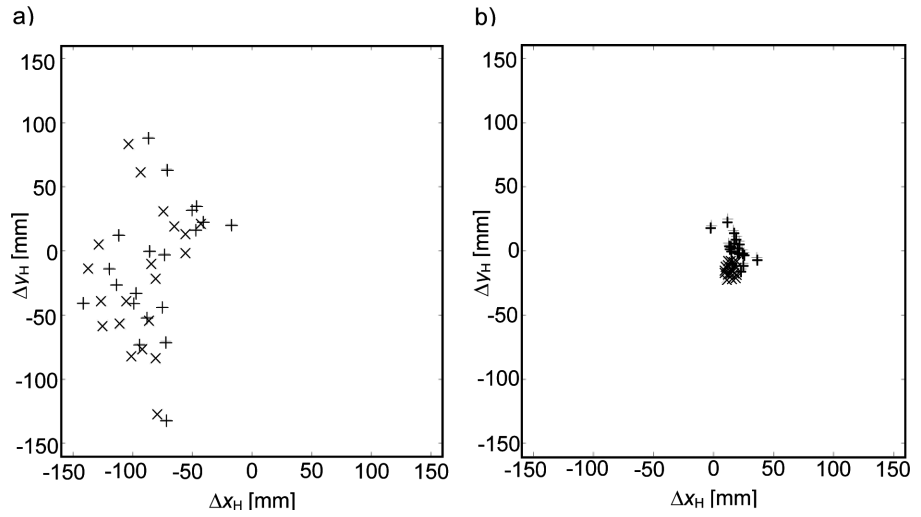

Fig. 11. Final positions of point H of the mobile platform: a) the PID control, b) optimal control at energy performance index, + direct measurement, × incremental measurement with a use of the platform's encoders

5. Conclusion

The essence and importance of surveillance of dynamic processes is emphasised in the scope of the chosen mechatronic systems. The latter concerns processes of the high speed milling vibration reduction, as well as – the mobile platform motion control. The authorial method of optimal control at energy performance index is applied for this purpose. The method is especially dedicated to surveillance of various discrete structures. Advantage of the method of surveillance is evidenced by theoretical derivations, computer simulations, as well as – by experiments made in case of real target objects and operation processes.

The presented considerations, in particular – the results of computer simulations and experimental investigations, allow us to formulate conclusions concerning efficiency of the self-excited chatter vibration surveillance method, applied in high-speed slender milling of various rigid details. The method of optimal-linear spindle speed control appeared to be successful in the application to reduction of the vibration level RMS, as well as – the chatter vibration amplitude. The quality of the machined surface, under vibration surveillance, is also improved during the process performance. Chatter vibration surveillance in modern milling centres has a great practical meaning. The reason is that the development of modern design solutions for the machining centres and application of reliable cutting tools causes that the cutting process itself remains the weakest link in the milling system.

Optimal control at energy performance index appeared to be an effective method of motion surveillance in the strongly nonliner system. The method's effectiveness is demonstrated on the example of a two-wheeled mobile platform. Efficiency of the proposed method is confirmed by the results of computer simulations and experimental investigations in the case of the selected paths of a motion. The results of platform motion surveillance, obtained with the use of the proposed method of the optimal control, present much better quality than the results achieved by using the PID controllers. There errors of position and orientation of the platform generated during its motion are significantly reduced. Repeatability of the desired target position is visibly improved, as well.

Manuscript received by Editorial Board, November 27, 2012;
final version, February 10, 2013.

REFERENCES

[1] Gawroński W.: Dynamics and control of structures – A modal approach. New York, Springer, 1999.

[2] Górecki H., Fuksa S., Korytowski A., Mitkowski W.: Sterowanie optymalne w systemach liniowych z kwadratowym wskaźnikiem jakości (Optimal control in linear systems at quadratic performance index). Warszawa, PWN, 1983.
[3] Jezequel L., Roberti V.: Optimal preview semiactive suspension. Transactions of the ASME Journal of Dynamic Systems Measurement and Control, 1996, Vol. 118, March, 99-105.
[4] Kaliński K.: Nadzorowanie drgań układów mechanicznych modelowanych dyskretnie (Vibration surveillance of mechanical systems which are idealised discretely). Gdańsk, Wydawnictwo PG, 2001. ISBN 83-88007-83-1.
[5] Tou J.T.: Nowoczesna teoria sterowania (Modern control theory). Warszawa, WNT, 1967.
[6] Engel Z., Kowal J.: Sterowanie procesami wibroakustycznymi (Control of vibroacoustic processes). Kraków, Wydawnictwa AGH, 1995. ISSN 0239-6114.
[7] Marchelek K.: Dynamika obrabiarek (Dynamics of machine tools). Warszawa, WNT, 1991.
[8] Tomków J.: Wibrostabilność obrabiarek (Vibrostability of machine tools). Warszawa, WNT, 1997.
[9] Xiao M., Karube S., Soutome T., Sato K.: Analysis of chatter suppression in vibration cutting. International Journal of Machine Tools and Manufacture, 2002, Vol. 42, No. 15, pp. 1677-1685.
[10] Mei Z., Yang S., Shi H., Chang S., Ehmann K.F.: Active chatter suppression by on-line variation of the rake and clearance angles in turning–principles and experimental investigations. International Journal of Machine Tools and Manufacture, 1994, Vol. 34, No. 7, pp. 981-990.
[11] Shiraishi M., Yamanaka K., Fujita H.: Optimal control of chatter in turning. International Journal of Machine Tools and Manufacture, 1991, Vol. 31, No. 1, pp. 31-43.
[12] Ganguli A., Deraemaekar A., Horodinca M., Preumont A.: Active damping of chatter in machine tools–demonstration with a "Hardware in the Loop" Simulator. Journal of Systems and Control Engineering, Proceedings of the Institution of Mechanical Engineers, 2005, Vol. 219, No. 15, pp. 359-369.
[13] Kim M.H., Won D., Ziegert J.: Numerical analysis and parameter study of a mechanical damper for use in long slender endmills. International Journal of Machine Tools and Manufacture, 2006, Vol. 46, pp. 500-507.
[14] Rashid M.K.: Simulation study on the improvements of machining accuracy by using smart materials. Robotics and Computer-Integrated Manufacturing, 2005, Vol. 21, pp. 249-257.
[15] Liao Y.S., Young Y.C.: A new on-line spindle speed regulation strategy for chatter control. International Journal of Machine Tools and Manufacture, 1996, Vol. 35, No. 6, pp. 651-660.
[16] Tarng Y.S., Lee E.C.: A critical investigation of the phase shift between the inner and outer modulation for the control of machine tool chatter. International Journal of Machine Tools and Manufacture, 1997, Vol. 37, No. 12, pp. 1661-1672.
[17] Soliman E., Ismail F.: Chatter suppression by adaptive speed modulation. International Journal of Machine Tools and Manufacture, 1997, Vol. 37, No. 3, pp. 355-369.
[18] Galewski M., Kaliński K.: Nadzorowanie drgań przy frezowaniu szybkościowym smukłymi narzędziami ze zmienną prędkością obrotową (Vibration surveillance at high speed slender milling with a use of changing spindle speed). Gdańsk, Wydawnictwo PG, 2009.
[19] Kalinski K.J., Galewski M.A.: Chatter vibration surveillance by the optimal-linear spindle speed control. Mechanical Systems and Signal Processing, 2011, Vol. 25, No. 1, pp. 383-399.
[20] Przemieniecki J.S.: Theory of Matrix Structural Analysis. Dover Publications, 1985.
[21] Kaliński K.J.: Nadzorowanie procesów dynamicznych w układach mechanicznych (A surveillance of dynamic processes in mechanical systems). Gdańsk, Wydawnictwo PG, 2012. ISBN 978-83-7348-448-1.
[22] Giergiel M.J., Hendzel Z., Żylski W.: Modelowanie i sterowanie mobilnych robotów kołowych (Modelling and control of wheeled mobile robots). Warszawa, PWN, 2002.
[23] Mazur M.: Nadzorowanie ruchu 2-kołowej platformy mobilnej z zastosowaniem sterowania

optymalnego przy energetycznym wskaźniku jakości, Praca doktorska (Motion surveillance of 2-wheeled mobile platform with a use of the optimal control at energy performance index Ph.D thesis), Politechnika Gdańska, Gdańsk, 2010.

Nadzorowanie procesów dynamicznych w wybranych układach mechatronicznych

S t r e s z c z e n i e

Artykuł poświęcony jest przedstawieniu oryginalnej metody sterowania optymalnego z wykorzystaniem energetycznego wskaźnika jakości i jej zastosowaniu do nadzorowania procesów dynamicznych w wybranych systemach mechatronicznych. W szczególności dotyczy to nadzorowania drgań *chatter* podczas obróbki szybkościowej przedmiotów sztywnych z wykorzystaniem narzędzi smukłych oraz sterowania ruchem dwukołowej platformy mobilnej. Rezultaty symulacji komputerowych oraz przeprowadzone badania eksperymentalne na rzeczywistych obiektach pokazują dużą efektywność proponowanej metody.